

Quasi Static Remanence in Dzyaloshinskii-Moriya Interaction driven Weak Ferromagnets and Piezomagnets

Namrata Pattanayak,¹ Arpan Bhattacharyya,² A. K. Nigam,³ Sang-Wook Cheong,⁴ and Ashna Bajpai^{1,5}

¹*Department of Physics, Indian Institute of Science Education and Research, Dr. Homi Bhabha Road, Pune 411008, India*

²*Saha Institute of Nuclear Physics, 1/AF Bidhannagar, Kolkata, India*

³*Department of Condensed Matter Physics and Material Science,*

Tata Institute of Fundamental Research, Dr. Homi Bhabha Road, Mumbai 400 005, India

⁴*Rutgers Center for Emergent Materials and Department of Physics and Astronomy,*

Rutgers University, Piscataway, New Jersey 08854, USA

⁵*Center for Energy Science, Indian Institute of Science Education and Research, Dr. Homi Bhabha Road, Pune 411008, India**

(Dated: September 14, 2021)

We explore remanent magnetization (μ) as a function of time and temperature, in a variety of rhombohedral antiferromagnets (AFM) which are also weak ferromagnets (WFM) and piezomagnets (PzM). These measurements, across samples with length scales ranging from nano to bulk, firmly establish the presence of a remanence that is quasi static in nature and exhibits a counter-intuitive magnetic field dependence. These observations unravel an ultra-slow magnetization relaxation phenomenon related to this quasi static remanence. This feature is also observed in a defect free single crystal of α -Fe₂O₃, which is a canonical WFM and PzM. Notably, α -Fe₂O₃ is not a typical geometrically frustrated AFM and in single crystal form, it is also devoid of any size or interface effects, which are the usual suspects for a slow magnetization relaxation phenomenon. The underlying pinning mechanism appears exclusive to those AFM which are either symmetry allowed WFM, driven by Dzyaloshinskii-Moriya Interaction (DMI) or can generate this trait by tuning of size and interface. The qualitative features of the quasi static remanence indicate that such WFM are potential piezomagnets, in which magnetization can be tuned by *stress* alone.

I. INTRODUCTION

Phenomenon of weak ferromagnetism in certain antiferromagnets, including the classic case of α -Fe₂O₃, is associated with the experimental observation of a ferromagnetic (FM) like, spontaneous moment. This feature was initially attributed to a FM impurity phase in an otherwise AFM lattice; such as Fe₃O₄ impurity in α -Fe₂O₃.¹⁻⁴ This controversy was firmly resolved by Dzyaloshinskii in 1958,¹ who proposed a spin canting mechanism that leads to a weak FM like state and Moriya⁴ who discovered the microscopic origin of this spin canting and its connection with spin orbit coupling (SOC). This is the celebrated Dzyaloshinskii-Moriya Interaction (DMI), of the type $\mathbf{D} \cdot (\mathbf{S}_i \times \mathbf{S}_j)$ which is now central to both fundamental and application based trends in contemporary condensed matter physics. Apart from exotic inhomogeneous spin textures and non collinear spin systems such as skyrmions, topological insulators and superconductors, DMI/SOC also brings into fore the role of antiferromagnetic insulators in spintronics.⁵⁻¹⁴

In many of the symmetry allowed weak ferromagnets, which include rhombohedral AFMs like α -Fe₂O₃, MnCO₃ and rutile AFMs like NiF₂ or CoF₂, the phenomenon of stress induced moments or piezomagnetism, of the type ($M_i = P_{ijk}\sigma_{jk}$) where σ is stress, was also predicted by Dzyaloshinskii.¹ Experimental observations of such stress induced moments were made by Borovik-Romanov in a variety of WFM/PzM single crystals in the seminal work spanning from 1960s to 70s.¹⁵⁻¹⁸ On the similar lines of magnetoelectricity, wherein a magnetic moment can be created by *electric field* alone - for which Cr₂O₃ is a prototype^{19,20} - magnetic moment from *stress* alone can occur in PzM, for which α -Fe₂O₃ is a prototype.^{19,21,22} It is also interesting that both Cr₂O₃ and

α -Fe₂O₃ are isostructural AFM but the piezomagnetic moments are observed in α -Fe₂O₃, not in bulk Cr₂O₃. A picture also emerged with a plausible explanation on the microscopic mechanism of PzM in these systems.^{23,24}

In some of these WFM/PzM compounds or in their doped versions,²⁵ an unusually slow magnetization relaxation was tracked through the measurement of remanence. This was further seen in ultra-thin films of Cr₂O₃,²⁶ in FM/AFM core shell systems where Cr₂O₃ appeared as an ultra-thin surface layer²⁷ and also when Cr₂O₃ is encapsulated inside carbon nanotubes²⁸ (CNT). These reports pointed towards some features in remanence which appear to be common, especially for AFM with the possibility of WFM/PzM. Most intriguing among these is ultra slow magnetization relaxation phenomenon, resulting in the observation of a quasi static remanence with a counter-intuitive magnetic field dependence.^{27,28}

Interestingly, Cr₂O₃ is not a symmetry allowed WFM/PzM but exhibits quasi static remanence only when it is in an ultra-thin form. It is therefore important to systematically explore whether these features intrinsically exist in symmetry allowed WFM and to investigate the circumstances in which this can appear in systems with altered symmetry conditions, especially due to size/interface effects. In addition, what still remains an open question is whether piezomagnetism will always co-exist in all WFM and if so, what are the foot prints of this phenomenon? It is also important to explore possible means to isolate this subtle effect from routine magnetization measurements, wherein all other field dependent processes contribute for any AFM (canted or otherwise) under magnetic field.

In this work we explore remanence in two rhombohedral AFM that are symmetry allowed WFM and PzM. This includes α -Fe₂O₃ with Neel transition temperature (T_N) \sim 950

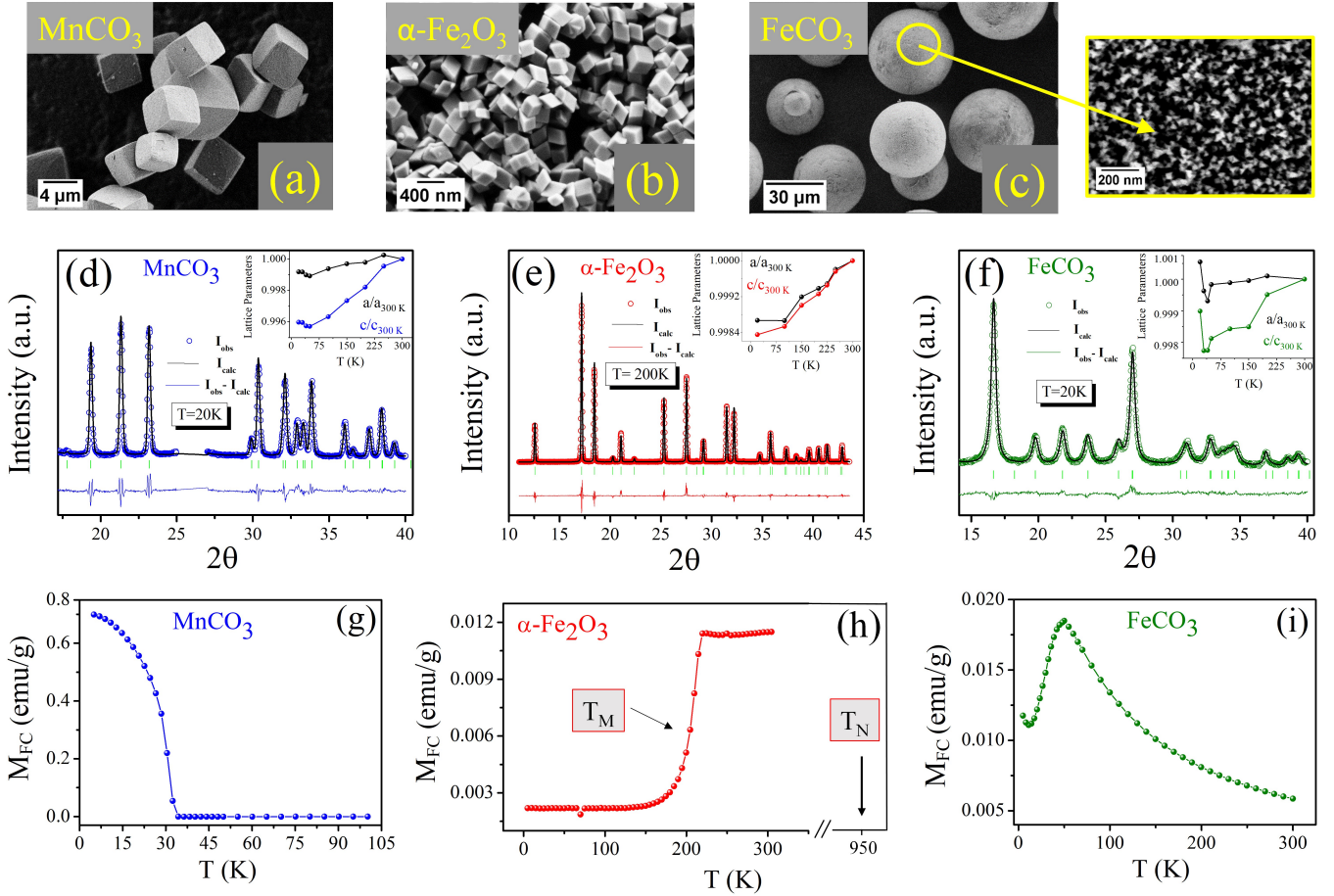


Figure 1. SEM images of (a) micro-cubes MnCO_3 , (b) nano-cubes $\alpha\text{-Fe}_2\text{O}_3$ and (c) FeCO_3 spheres with diameter $\sim 20 \mu\text{m}$. Each sphere consists of triangular FeCO_3 nano particles $\sim 5\text{-}10 \text{ nm}$. Figures (e)-(f) display Synchrotron XRD data of MnCO_3 $\alpha\text{-Fe}_2\text{O}_3$ and FeCO_3 along with Rietveld fitting. The inset shows best fit lattice parameters derived from Rietveld profile refinement of I vs 2θ data recorded at different temperatures. The magnetization as a function of temperature from 300 K to 5K in presence of $H = 1 \text{ kOe}$ for all three samples is shown in figures (g)-(i). For MnCO_3 and FeCO_3 , the Neel transition temperature is 30 K and 50 K respectively as evident from (g) and (i) respectively. For $\alpha\text{-Fe}_2\text{O}_3$, the Morin transition T_M signifying spin re-orientation transition from WFM to pure AFM state is around 260K. The actual Neel transition is around 950 K, shown schematically in (h).

K and MnCO_3 with $T_N \sim 30 \text{ K}$. Here $\alpha\text{-Fe}_2\text{O}_3$ is known to be a pure AFM upto 260 K and a WFM in the temperature range of 260-950 K.^{1,16} The temperature at which $\alpha\text{-Fe}_2\text{O}_3$ becomes WFM/PzM is also known as Morin Transition, T_M ($\sim 260 \text{ K}$). It is advantageous to have a WFM near the room temperature for practical applications. However the effect is known to be much weaker than MnCO_3 .¹ We also investigate isostructural compound FeCO_3 with $T_N \sim 50 \text{ K}$, for which there are conflicting reports in literature about the existence of WFM and PzM.^{1-3,17} For such cases, size effects may play a prominent role as DMI can be dominant and enhanced at surfaces and interfaces.²⁹

We study all three samples in the form of nano and mesoscopic crystals / particles and show a correlation between the structural parameters and the magnitude of pinned moment related to the quasi static remanence. In case of $\alpha\text{-Fe}_2\text{O}_3$, which is also a prototypical PzM near the room temperature, we confirm the ultra slow magnetization relaxation in its single crys-

tal form, thus bringing out that the quasi static remanence is intrinsic. We also show that this feature can be substantially tuned by size effects, by comparing the magnitude of quasi static remanence in the single crystal and nano cubes of $\alpha\text{-Fe}_2\text{O}_3$.

II. EXPERIMENTAL TECHNIQUES

Micro-cubes of MnCO_3 (length $\sim 2\text{-}4 \mu\text{m}$), nano-cubes of $\alpha\text{-Fe}_2\text{O}_3$ (length $\sim 200 \text{ nm}$) and polycrystalline spheres of FeCO_3 (grain size $\sim 5\text{-}10 \text{ nm}$) have been synthesized following the precipitation and hydrothermal routes³⁰⁻³² Fig.1a-1c. The single crystal of $\alpha\text{-Fe}_2\text{O}_3$ has been grown using Floating Zone technique. Scanning Electron Microscopy images are recorded using ZEISS ULTRA plus field-emission SEM. All the samples have been characterized using X-ray powder diffraction (XRD) using Bruker D8 Advance with $\text{Cu K}\alpha$ ra-

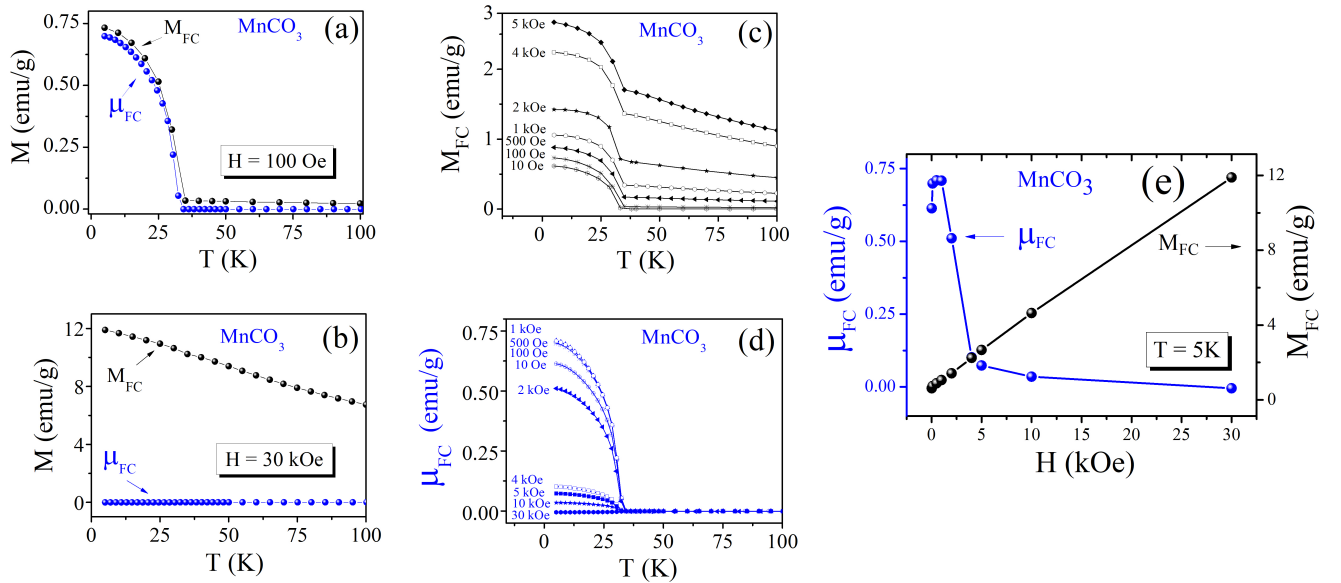


Figure 2. Black dots in (a) show magnetization measured while cooling ($H = 100$ Oe) and blue dots are corresponding remanence ($H=0$) measured while warming for MnCO_3 sample. (b) shows the same for $H=30$ kOe. (c) M_{FC} vs T at various H depicting regular AFM behavior with M_{FC} rising with rise in H . (d) shows corresponding μ_{FC} vs T exhibit s strikingly different cooling H dependence. (e) compares the magnitude of M_{FC} (black dots, right axis) and μ_{FC} (blue dots, left axis) at 5K as a function of (cooling) H for MnCO_3 .

Sample	a (Å)	c (Å)	c/a
MnCO_3	4.7723(7)	15.611(3)	3.27
FeCO_3	4.6678(4)	15.202(1)	3.25
$\alpha\text{-Fe}_2\text{O}_3$	5.0087(1)	13.6856(4)	2.73

Table I. Structural Parameters of MnCO_3 , $\alpha\text{-Fe}_2\text{O}_3$ and FeCO_3 as determined from the Rietveld analysis of room temperature X-ray diffraction data.

radiation ($\lambda = 1.54056$ Å). (Supp. Info : Fig. S1-S3). Temperature variation of synchrotron XRD from 20 K-300 K has been conducted in BL-18 beam line, Photon Factory, Japan. The synchrotron XRD data has been fitted using Rietveld Profile Refinement. All three samples stabilize in rhombohedral structure and fitting has been done in hex setting. The XRD data along with the Rietveld fittings at few selected temperatures for each of the sample is shown in Fig. 1d-1f. The refined lattice parameters a and c at room temperature for all three samples are given in table 1. The Temperature variation of refined lattice parameters a and c for the samples are shown in the respective insets in Fig. 1d-1f. Here both a and c are normalized with their respective room temperature value. The magnetization measurements have been carried out by using a superconducting quantum interference device (SQUID) magnetometer, Quantum Design MPMS-XL.

III. RESULTS AND DISCUSSIONS

Magnetization as a function of Temperature (M_{FC} vs T) recorded while cooling in presence of magnetic field $H = 1$

kOe is presented Fig. 1g-1i for all three samples. This is the routinely known Field Cooled (FC) cycle. The Neel transition temperature for MnCO_3 and FeCO_3 as shown in Figure 1, match well with the respective literature values. For both these samples, the H is applied in the paramagnetic region, prior to the FC cycle. However, for $\alpha\text{-Fe}_2\text{O}_3$, the T_N is 950 K and it is marked schematically in the 1h. This is to indicate that in the case of $\alpha\text{-Fe}_2\text{O}_3$, the magnetization data is recorded while cooling from 300 K, which is above its Morin Transition temperature (T_M) but below its Neel temperature (T_N). For single crystal of $\alpha\text{-Fe}_2\text{O}_3$, the magnetization (M_{ZFC}) is also recorded in Zero Field Cooled (ZFC) state as would be shown in the latter part of the text. These factors have important implications while preparing a remanent state for all these samples considered here.

A. Preparation of the Remanent State : FC/ZFC protocol

Our primary tool here is DC magnetization in remanent state.³³⁻³⁹ This enables us to track the magnetization relaxation phenomenon and hence pinning potential landscape in all these WFM. This remanent state is prepared in two experimental protocols, the FC and ZFC.

In FC protocol, the sample is cooled in a specified magnetic field, H , which is applied much above the T_N (or T_M) and the M_{FC} is recorded while cooling. The H is switched off at 5K, and thereafter the remanent magnetization (or remanence) is experimentally measured in $H = 0$ state. This remanence, prepared after a typical FC cycle, is referred to as μ_{FC} . This can be measured either (i) as a function of increasing temperature from 5K to 300 K or (ii) as a function of time

at 5K.

In the ZFC protocol, employed only for the single crystal of α -Fe₂O₃, the H is applied from below the T_M and M_{ZFC} is measured in warming cycle, right upto 300 K. Thereafter H is switched off and the corresponding remanence, referred to as μ_{ZFC} , is measured as a function of *time* at 300 K.

We emphasize that in all the subsequent data involving μ presented in this work, the magnitude of H indicated in the plots refers to the magnetic field applied during either cooling or warming cycle, so as to **prepare** a remanent state. This remanence (μ_{FC} or μ_{ZFC}), the origin of which is the subject matter of investigation here, is experimentally measured only after switching *OFF* the H .

B. Temperature Variation of Remanence in MnCO₃

Fig.2a shows M_{FC} vs T , (measured while cooling) in presence of $H \sim 100$ Oe (black dots). The magnitude of M_{FC} at 5K ~ 0.75 emu/g. After removal of H at 5K, a part of the magnetization decays instantaneously. However, a significant part of magnetization remains pinned, resulting in the observation of remanence. This remanence (μ_{FC}) shows almost no further decay as a function of time, as long as the temperature is held constant at 5K. As evident from Fig.2a, the magnitude of the μ_{FC} at 5K is ~ 0.7 emu/g for this run. On increasing the temperature, μ_{FC} vs T (measured while warming) shows a variation which is qualitatively similar to M_{FC} vs T right up to the T_N as shown in Fig.2a (blue dots). In the paramagnetic tail, the μ_{FC} vanishes, as is expected.

Fig.2b shows the same for $H \sim 30$ kOe, for which $M_{FC} \sim 12$ emu/g whereas the $\mu_{FC} \sim 10^{-5}$ emu/g at 5 K. Thus the μ_{FC} is vanishingly small for 30 kOe run. We would consider the μ of this magnitude to be roughly arising from the quenched field of SQUID superconducting magnet, which may be ~ 5 -10 Oe and can vary from run to run⁴⁰. The data contained in Fig.2 clearly indicates that the magnitude of μ is almost equivalent to that of M_{FC} for lower (cooling) H whereas it is negligible for very high H .

For all the intermediate magnetic fields, the M_{FC} vs T data are plotted in 2c and their corresponding μ_{FC} vs T are plotted in Fig.2d. As is evident from these data, the magnetization increases with increasing H , consistent with a regular AFM behaviour. However, the corresponding remanence varies with the strength of the magnetic field in an unexpected way. Here the remanence is first seen to rise with increasing H , upto a critical field. Thereafter it decreases with increase in field and eventually vanishes beyond another critical field.

To clearly bring out the unusual (cooling) field dependence of the μ_{FC} , we compare the magnitude of both M and μ at 5K. These data points are extracted from different M_{FC} vs T and their corresponding μ_{FC} vs T runs Fig.2e. Here M_{FC} is seen to increase with increasing H , as is expected for a regular AFM, whereas the μ_{FC} initially rises with increasing H , followed by a sharp drop. The μ_{FC} completely vanishes at very high field. The type of field dependence of μ is not expected for either a regular FM or AFM.³⁴⁻³⁶ Thus the H dependence of the remanence (blue dots) brings forward a

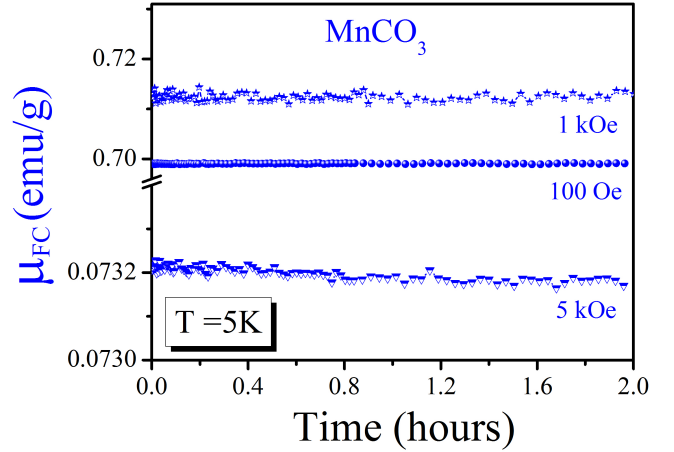


Figure 3. Remanence as a function of time for three different cooling fields at a fixed temperature of 5K for MnCO₃. These data show that the remanence is almost constant over a time period of 2 hours, thus depicting its quasi static nature.

unique functional form, which is not observed in the routine M vs H isotherm (black dots).

C. Remanence in MnCO₃: Variation with Time

To check the stability of the remanence as a function of time, we also performed relaxation rate measurements. After a typical M_{FC} vs T and subsequent removal of H , we obtained μ_{FC} vs *time*, while the temperature is held constant at 5K (Fig.3). These remanence data, obtained for three different cooling fields, again brings forward two distinct magnetization relaxation rate, one of which is ultra-slow. We observe that for measurement times of about two hours, the μ_{FC} shows no appreciable decay and this type of remanence can be termed as quasi static in nature.

Consistent with the data presented in Fig.2d, magnitude of the μ_{FC} is seen to vary with cooling field H in a way, which is not obvious from the routine temperature M - H isotherms. For the chosen cooling fields of 100 Oe, 1 kOe and 5 kOe, the μ_{FC} values are $\sim 93\%$, 70% and 3% of their corresponding M_{FC} values. These data also indicate that finding an optimum value of the (cooling) magnetic field enables almost all the in-field magnetization to be retained. For instance, the remanence corresponding to 100 Oe run is 93% of its M_{FC} value. However, even for the run corresponding to 5 kOe, for which the magnitude of remanence is about 3% of its M_{FC} value, the relaxation rate is still ultra slow. Thus the data contained in Fig.3 confirms presence of the remanence that is quasi static in nature with ultra-slow magnetization dynamics, and exhibits a counter intuitive H dependence (Fig.2e).

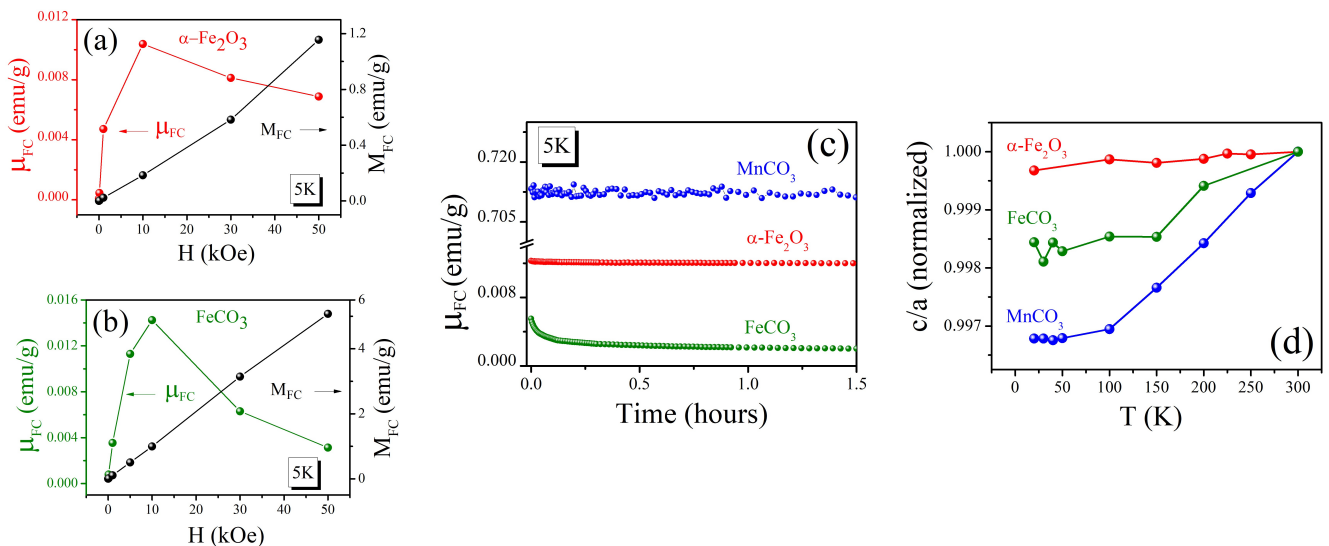


Figure 4. (a) and (b) shows μ_{FC} as a function of (cooling) H for $\alpha\text{-Fe}_2\text{O}_3$ and FeCO_3 respectively. The corresponding M vs H is shown for each sample is shown in the same graph, indicating the unusual (cooling) field dependence of remanence for both the samples. (c) Compares μ_{FC} as a function of *time* in all three samples. The observation of the quasi static nature of remanence is unambiguous in case of MnCO_3 as well as $\alpha\text{-Fe}_2\text{O}_3$. (d) shows c/a ratio using refined lattice parameters obtained at various temperature from Rietveld fitting of synchrotron XRD data. The c/a ratio has been normalized with its value at 300 K.

D. Remanence and structural parameters in $\alpha\text{-Fe}_2\text{O}_3$, FeCO_3 and MnCO_3

Similar measurements were also conducted for $\alpha\text{-Fe}_2\text{O}_3$ and FeCO_3 samples. Fig.4a and Fig.4b displays μ_{FC} vs H data at 5K (extracted from various μ_{FC} vs T runs) for both the samples. These data reveal that the μ_{FC} vs H for each of the sample is strikingly different from corresponding M_{FC} vs H shown on the right axis in each plot. Both the samples exhibit a sharp rise in μ_{FC} as a function of (cooling) H and the peak value of μ is obtained at different critical H for each sample. This rise is qualitatively similar to what is seen for MnCO_3 (Fig.2e), though the fall, after the peak is not as rapid. Overall, the field dependence of remanence is counter-intuitive in all three samples.

In addition, all three samples exhibit two distinct time scales for magnetization decay, one of which is ultra slow and can be termed as quasi static. This slow magnetization relaxation is evident in μ_{FC} vs time measurements as shown in Fig.4c. For sake of comparison, for each sample the remanent state is prepared in cooling magnetic field of 1 kOe. The magnitude of the remanence is atleast an order of magnitude higher for MnCO_3 as compared to $\alpha\text{-Fe}_2\text{O}_3$. This is also consistent with the earlier observations which indicate that the net FM moment due to spin canting is about an order of magnitude larger larger in MnCO_3 .¹

To correlate the observed features in μ with structural parameters, the temperature variation of a and c lattice parameters is studied. As can be seen from the inset of Fig.1d, for MnCO_3 , both a and c decrease with reducing temperature monotonically till about the T_N , however an expansion in both the lattice parameters is observed just below its AFM transi-

tion temperature. In addition, for MnCO_3 the lattice parameter c is seen to fall much rapidly with reducing temperature as compared to a (inset of Fig.1d). On the contrary, for $\alpha\text{-Fe}_2\text{O}_3$, the pattern of temperature variation for c and a are quite similar in nature and a slight trend of expansion in both lattice parameters is observed around its WFM region (Fig.1e). For all three samples, both lattice parameters exhibit a slight anomaly below T_N (or around WFM in case of $\alpha\text{-Fe}_2\text{O}_3$), however the effect is more pronounced for the MnCO_3 .

Fig.4d compares normalized c/a ratio as a function of temperature for all three samples. This normalization is w.r.t c/a ratio at 300 K for each sample. We find that the c/a ratio shows a more rapid decline with reducing temperature and a clear anomaly is observed in the WFM region for MnCO_3 . This trend also correlates with the stability and magnitude of the μ , both of which are relatively higher for MnCO_3 as compared to $\alpha\text{-Fe}_2\text{O}_3$. In case of FeCO_3 , though the qualitative features in remanence are similar, but the morphology of the sample makes its difficult to conclude whether these features are intrinsic or arising due to nano scaling. In this case, the grain size is of the order of 2-5 nm, Fig.1c. This situation is similar to what is observed for Cr_2O_3 which is also isostructural with $\alpha\text{-Fe}_2\text{O}_3$ but it is not symmetry allowed WFM in bulk. However, it exhibits slow relaxation and the unusual cooling field dependence of remanence only in ultra thin form.^{27,28} Microscopic measurements are needed to confirm the presence of WFM in such cases, including ultra small FeCO_3 grains used in this study.

For physical mechanism related to the remanence that results in ultra-slow magnetization relaxation, a number of phenomena such as glassy phase, superparamagnetism, defect pinning in a regular FM or AFM, exchange bias at FM/AFM

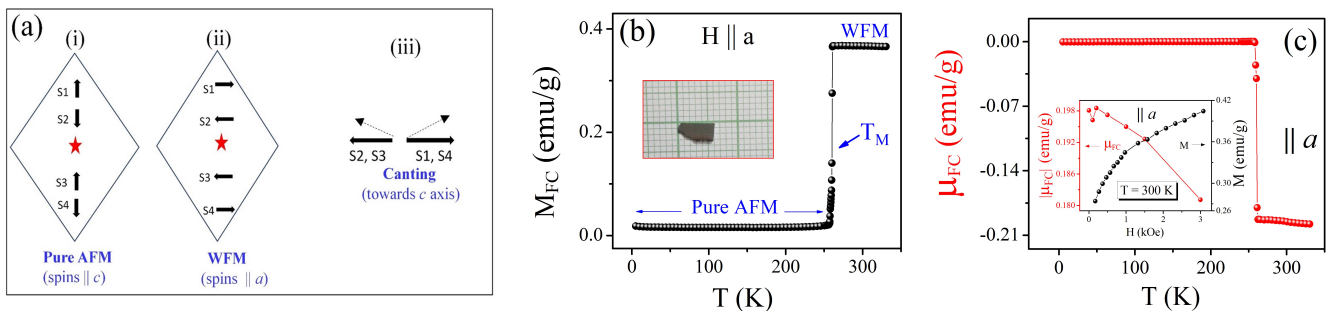


Figure 5. (a) shows schematic of typical spin configurations in pure AFM (i) and WFM (ii) phase along with the phenomenon of canting (iii). The red star in (i) is the inversion center and the spins point along the c axis in pure AFM phase. In WFM phase, spin tilt in basal plane as shown in (ii). The spin configuration shown in (ii) is necessary for the observation of DMI driven spin canting that results in WFM phase. (b) M_{FC} vs T for a single crystal of α -Fe₂O₃, with H (1kOe) parallel to a axis, exhibiting T_M , the Morin transition, marked as blue arrow in the figure. The inset shows the picture of the α -Fe₂O₃ single crystal. (c) shows μ_{FC} vs T run corresponding to the M_{FC} vs T run shown in (b). Here the remanence is vanishingly small in the pure AFM region and finite in the WFM region. The inset shows μ_{FC} at 300 K along a axis as a function of various (cooling) H . These data points are extracted from various μ_{FC} vs T runs.

interface etc. can be considered. Such phenomena are known to result in slow relaxation with a variety of temporal functional forms.^{33–38} However the mechanism behind the quasi static remanence and its unusual (cooling) magnetic field dependence in these samples appears to be different from above mentioned phenomena. For instance, considering size effects, MnCO₃ shows most robust magnetization pinning at lower fields, as shown in Fig.3. However, the sample used for magnetization measurements consists of fairly big crystallites (~ 2 -4 μ m) therefore it is less likely that the slow relaxation is arising from size reduction or nano scaling. It is neither a glassy system, nor a nano scale FM which can exhibit superparamagnetic traits. Crystallites are also regular shaped with well-formed facets therefore the phenomenon of defect pinning leading to ultra-slow magnetization relaxation is ruled out. Also, for a regular AFM/FM, the μ should have shown saturation³⁴ with H , rather than the sharp drop such as seen in Fig.2e.

To understand the nature of remanence in AFM with WFM traits and to confirm if this effect is intrinsic, we also explored it in a single crystal (SC). For this purpose, we chose a SC of α -Fe₂O₃ as this sample is well known to exhibit a spin reorientation transition from pure AFM to WFM phase.¹

E. Pure AFM and WFM Phase : Symmetry Considerations

Among the samples considered here, α -Fe₂O₃ is known to be both pure AFM (upto 260 K) and WFM (260 K - 950 K).¹ Here pure AFM phase implies that the DMI driven spin canting is not symmetry allowed. As mentioned before, isostructural compound Cr₂O₃ which does not exhibit spin canting, in this context, is a pure AFM phase.¹ For the sake of clarity, the spin configurations in pure-AFM and WFM state are compared in Fig.5a. In pure AFM phase, the spins within unit cell are arranged along c axis as shown in Fig.5a, configuration (i). Here the red star is the inversion center and the spin configuration can be $S1 = -S2 = S3 = -S4$ as shown in (i). In WFM state,

the spins re-orient to the basal plane, arranged in a specific sequence, in which $S1 = -S2 = -S3 = S4$. It is important to note that the unit cell is still AFM, but the spin configuration shown in (ii) is essential for DMI driven spin canting. This $\mathbf{D} \cdot (\mathbf{S}_i \times \mathbf{S}_j)$ type of interaction is possible between sub-lattices associated with antiferromagnetically coupled spins, with the sign of D consistent with the symmetry considerations discussed in references 1-4. The direction of the net FM moment due to the spin canting is towards the c direction as is shown schematically in Fig.5a(iii). This net FM moment in **otherwise AFM** is responsible for **weak ferromagnetism**.

The spin configurations shown in Fig.5a(ii) is valid for all the rhombohedral AFM discussed here, which are symmetry allowed WFM. For α -Fe₂O₃, the spin reorientation transition from pure AFM (spins along c axis) to WFM state (spins along a axis) occurs at T_M , the Morin transition temperature.¹ Thus α -Fe₂O₃ provides a unique opportunity to probe both AFM and WFM phase in the same sample, which individually exist in a wide temperature range. In the following, we present results of remanence measurements in the single crystal of α -Fe₂O₃ in both the regions.

F. Remanence in a Single Crystal of α -Fe₂O₃ : Variation with Temperature

Main panel of Fig.5b shows M_{FC} Vs T for a SC of α -Fe₂O₃ sample along a axis. The Morin transition at ~ 260 K demarcates the two regions, pure AFM and WFM for this sample. From this, we note that magnitude of M_{FC} is roughly ~ 0.35 emu/g in WFM region and ~ 0.015 emu/g in the pure AFM region. After switching off the field at 5K, corresponding μ_{FC} vs T in warming cycle is shown in the main panel of Fig.5c. The μ_{FC} is found to be negligibly small (10^{-5} emu/g) in the pure AFM region and substantially large in WFM region (-0.2 emu/g).

Here, the sign of the μ_{FC} is found to be negative w.r.t the direction of applied H . From a number of such μ_{FC} vs T data

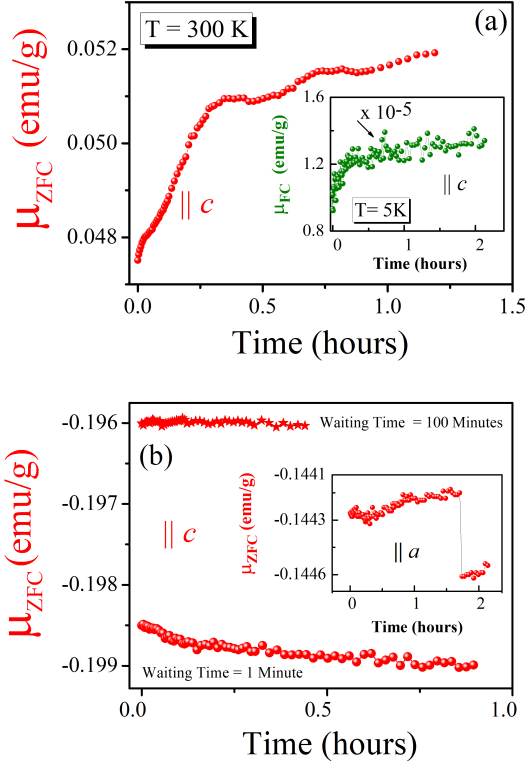


Figure 6. (a) shows μ_{ZFC} vs time at 300 K (WFM region) measured along the c axis for the single crystal of α - Fe_2O_3 . The inset shows μ_{FC} vs time along c axis at 5K (pure AFM region). While μ_{FC} is negligibly small in the pure AFM region, it is substantially large (at-least by a few orders of magnitude) in the WFM region. (b) Main panel shows μ_{ZFC} vs time measurements parallel to c axis for waiting time of 100 minutes (red stars) and 1 minute (red dots). Inset shows μ_{ZFC} vs time parallel to a axis showing discrete jump.

along a axis, we find that the sign of μ_{FC} at 300 K remains primarily negative and its magnitude shows a slight decrease with increasing magnetic fields (inset in Fig.5c). It is to be noted that for obtaining this data, the H during FC cycle is applied at 300 K, when the sample is in WFM region. This is unlike the case of MnCO_3 , where the H can be applied in the paramagnetic region. For obtaining the (cooling) field dependence of remanence unambiguously, such as shown in Fig.2e for MnCO_3 , it is preferable to apply the H in the paramagnetic region for preparing individual remanent states. However, in case of α - Fe_2O_3 , it is not practically possible to heat the sample above 950K, after each run. Though the sign of the μ_{FC} along a axis is not commensurate with the direction applied H while cooling, its magnitude is substantial only in WFM region.

To check the stability of this remanence as a function of time, we conducted relaxation measurements both along the c as well as a axis. Since the direction of net FM moment is likely to be towards the c axis of the crystal, we particularly checked stability of μ_{ZFC} as well as μ_{FC} along c axis as a function of time.

G. Remanence in a Single Crystal of α - Fe_2O_3 : Variation with Time

In this section we present relaxation rate of remanence in pure AFM and WFM phase of α - Fe_2O_3 , measured following the FC and ZFC protocol respectively.

For remanence in the pure AFM region, the H is applied from 300 K and M_{FC} vs T is recorded while cooling (not shown here). The H is switched off at 5K and the μ_{FC} is measured as a function of time. This is shown in the inset of Fig.6a. These data further confirm that the remanence is negligible in pure AFM region $\sim 10^{-5}$ emu/g (inset of Fig.6a).

For preparing the remanent state in WFM region, the H is applied from below the T_M and M_{ZFC} vs T is recorded while warming, right upto 300 K (not shown here). At 300 K, the H is switched off and μ_{ZFC} is measured as a function of time (main panel, Fig.6a). Here, the remanence is positive and is commensurate with the direction of H applied during ZFC cycle. Thus the remanence is substantial in magnitude in WFM region and it is also fairly stable in time.

However, from a number of μ_{ZFC} vs time cycles in positive H , we observe that the magnitude of μ_{ZFC} in WFM region varies from 0.05-0.2 emu/g but its sign primarily remains negative. This anomaly appears only in the remanence measurements but not in the regular in-field measurements such as shown in Fig.5b. However, such ambiguity with sign has also been observed in the sign of stress induced moments in some WFM/PzM on repeated cooling.¹⁵ The reason for such ambiguity in case of remanence, (which does not appear in regular *in-field* magnetization) is also discussed in the latter part of the text. We also note a slight variation (5%) in the magnitude of μ , from run to run, for the same (cooling) magnetic field. These anomalies are also seen to appear only in the WFM region.

Interestingly, we also observe a slight trend of rise (\sim a few% of total remanence) in μ_{ZFC} vs time data, as shown in Fig.6a. The over all relaxation data appears to be a sum of both time-decay as well as time-rise of the remanence. This indicates that on application of H (while preparing the remanent state) the moments continue to reorient slowly in presence of H and on the removal of H , the time decay is ultra slow as well. This also indicates that the total time span in which the H is ON for preparing a particular remanent state is also an important parameter. This could also be responsible for variations in the magnitude of the remanence, as observed here. This result prompted us to perform *waiting time* dependence, usually employed for glassy systems.³⁷

For waiting time runs, two remanent states are prepared using the same (cooling) magnetic field. In first case, the $H = 1$ kOe is applied in ZFC protocol, from below the T_M and the sample is heated right up to 300 K. At 300 K the magnetic field was kept ON for waiting-time of 1 minute, prior to finally switching it OFF for the remanence measurements. The second remanent state is prepared following exactly the same protocol, however this time the $H = 1$ kOe is kept ON for waiting time of 100 minutes, prior to switching it OFF. These μ_{ZFC} vs time data parallel to c axis are presented in the main panel of Fig.6b, for 1 min (dots) or 100 min (stars) waiting-

time respectively. These data clearly indicate that the magnitude of the remanence also changes with the total time span of the H applied for preparing a particular remanent state. This also explains the slight differences in the magnitude of remanence from run to run. The inset shows the same for μ_{ZFC} parallel to a axis after 100 min of waiting time. Along the a axis, the magnetization relaxation is ultra slow and occasionally discrete jumps in remanence are observed, though the change is less than a percent. However, the remanence continues to exhibit quasi static nature.

These anomalies which exist in the remanent state are not observed in routine M vs T measurements. α -Fe₂O₃ is not a frustrated AFM and in the single crystal form, size/interface related phenomena cannot account for the *waiting time* effects and ultra-slow magnetization dynamics. From the observation of quasi static remanence in single crystal, together with similar features observed in MnCO₃, we conclude that the ultra-slow magnetization dynamics can be taken as indicative of the presence of WFM. This ultra-slow dynamics also appears to be associated with the microscopic details of the AFM domain which turn WFM due to spin canting.

H. Quasi static Remanence and DMI driven Spin Canting

Considering the microscopic reason for quasi static remanence (that leads to the ultra-slow magnetization dynamics as observed here) in these systems, we recall the details of magnetic structure in all these compounds. The spin arrangement shown in Fig.5a(ii) is essential for the observation of WFM. This should also limit the possible ways in which an AFM domain can exist in the WFM region. For a regular AFM, on the application of the H , the induced magnetization is driven by the Zeeman energy and the magnetocrystalline anisotropy. However, the additional factor in WFM will include response from *spontaneously* canted spins, related to the DMI as well. On removal of H , the reversal of the WFM domain will have to be accompanied by the reversal of the AFM moment which is energetically unfavorable.¹⁵ Once a AFM domain with spin-canting is formed, guided by a cooling H applied from above the AFM to PM transition, it is energetically unfavorable for these domains to relax, when the H is removed. This feature is only observed upto a critical value of H which can vary depending on the sample, as is observed here (Fig.3 and Fig.4a). Beyond a critical H , the magnetization dynamics is driven by Zeeman and magnetocrystalline anisotropy. The magnetization relaxation in this case is much faster, similar to what is observed for a normal AFM. However, below this critical field strength, the WFM domain configuration is guided by the sign of H field, when, it is applied from $T \gg T_N$. When the H is applied in WFM region, the spins are already spontaneously canted. This also explains the ambiguity with sign, as observed in case of α -Fe₂O₃.

For further confirming that the ambiguity with sign is related to spontaneous spin canting related with DMI and not arising due to measurement related artifacts, we revert back to MnCO₃ which has a $T_N \sim 30$ K and H can be applied in the paramagnetic region. Fig.7 shows M_{FC} vs T data recorded

while cooling from above T_N , down to 5 K, in presence of $H = +100$ Oe (blue dots). At 5K the H is switched off and the quasi static remanence is observed, which is positive in magnitude as the WFM domain configuration is already guided by the $H = +100$ Oe. Temperature still held at 5K, we again apply $H = -100$ Oe and subsequent to this, the M vs T is measured in warming cycle (FH cycle) in presence of $H = -100$ Oe. As is evident from the data shown in Fig.7, once pinned in WFM state from above T_N by a positive H , the negative field cannot change the sign of pinned moment and therefore the sign of remanence. The measured magnetization in presence of $H = -100$ Oe while warming (black dots) is still positive and clearly a magnetic field applied in WFM region does not make any difference. Thus the observed magnetization is basically due to the presence of positive remanence, stabilized during previous ($H = +100$ Oe) FC cycle. This data explains the ambiguity related with the sign of remanence, especially when the H field is applied in WFM region.

Over all, these data confirm that the quasi static remanence is observed below a critical value of H in WFM and related to anisotropic exchange. At higher H , the interplay is between Zeeman and exchange energy, as is usually observed for a regular AFM. The ambiguity related with the sign of μ in single crystal of α -Fe₂O₃ is related with configuration of AFM domains in which the spins are spontaneously canted due to DMI, even in the absence of H . On cooling or heating in presence of H leads to stabilization of these canted AFM domains in different configurations, compatible with the interplay of various energy scales involved. This feature again indicates that the net moment related to quasi static μ is associated with net FM moment arising due to spontaneous spin canting in otherwise AFM.

I. Quasi Static Remanence and Piezomagnetism

A general consensus in the literature is PzM is connected with the transition from pure AFM to WFM state in an otherwise AFM and one of the mechanism that leads to the WFM state is associated with DMI.¹⁸ As mentioned before, the *stress* induced moments have already been experimentally measured in such WFM systems.¹⁵⁻¹⁸ More importantly, the direction of net FM moment in the WFM phase is seen to coincide with the direction of PzM.¹⁵ It is also to be recalled that waiting-time effects and ambiguity with sign (similar to what is observed in remanence data for α -Fe₂O₃ w.r.t the sign of the applied H) have also been observed in the sign of stress induced moments in WFM/PzM on repeated cooling.^{15,21}

The data presented in Fig.7 explains the ambiguity with the sign and the robustness of the pinned moments in WFM region. The presence of quasi static remanence also shows that once the WFM domains have been formed, guided by the magnetic field from above the magnetic transition temperature, removal of H (or reversing its sign) does not make any difference. The net FM moment arise due to DMI driven canting, their direction can be manipulated only when the H is applied from above T_N . It is also well known that magnetization reversal in piezomoments would require the reversal

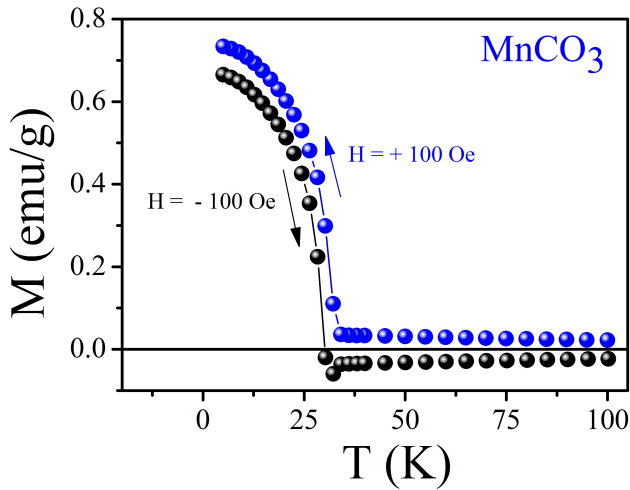


Figure 7. M Vs T recorded while cooling in presence of $H = +100$ Oe (blue dots). At 5K, the $H = +100$ Oe is removed and $H = -100$ Oe is applied while the temperature is held constant at 5K. Subsequently M vs T in presence of $H = -100$ Oe is again recorded in warming cycle (black dots). The measured magnetization is basically the remanence prepared during the previous cooling cycle. Since the sample is already in the WFM state, the presence of $H = -100$ Oe is not sufficient to rotate the magnetization. The robustness of pinned moment, which leads to quasi static remanence, for MnCO_3 is evident from this data.

of WFM sublattice which is energetically unfavorable.¹⁷ In remanence measurements, this phenomenon is manifested in the form of ultra slow magnetization relaxation (and consequently the quasi static remanence) as observed here. These data presented in Fig.2 to Fig.7 connect WFM and quasi static remanence. These data also further confirm that WFM phase is intimately related with the onset of transverse PzM in rhombohedral AFM.

We emphasize that the remanence data shown here not only bears a striking similarity with experimentally measured stress induced moments but also reveals features which are not obvious in routine in-field magnetization data. Thus it appears that the remanence measurements capture the essential physics of DMI driven WFM better than routine M vs T or M vs H and the onset of quasi static remanence can be taken as footprints of WFM and PzM.

From present data it also appears that ultra-slow magnetization dynamics and its unusual magnetic field dependence arises from the WFM and such systems are potential PzM. The magnitude of the WFM/PzM is further related to lattice parameters, especially c/a ratio in all these rhombohedral systems. A systematic study of such canonical WFM/PzM such as presented here, points towards the footprints of this phenomenon by simple magnetization measurements. It is to be emphasized that the system considered here are AFM with WFM trait. These are not frustrated AFM or a disordered glassy system / spin glass in conventional sense, which can exhibit slow relaxation for various other reasons. Therefore it is very interesting to observe ultra-slow relaxation in a completely ordered system in which these features are correlated

with DMI/SOC.

From our data, it can be concluded that for micro-cubes of MnCO_3 and nano-cubes and single crystal of $\alpha\text{-Fe}_2\text{O}_3$, the presence of ultra-slow magnetization dynamics is associated with intrinsic WFM. The temperature variation of remanence data on nano-cubes (Fig.4a) and single crystal of $\alpha\text{-Fe}_2\text{O}_3$, (Fig.5c) especially bring out that the magnitude of quasi static remanence can be significantly tuned by nanoscaling, as also has been observed earlier.^{27,28} For FeCO_3 , data is not sufficient to conclude whether effect is intrinsic or it is arising from the size reduction, as the sample comprises of 5-10 nm particles of FeCO_3 . In such cases, the strain in lattice parameters can also stabilize the WFM phase,²⁶⁻²⁸ however microscopic measurements are needed to confirm the presence of DMI driven canting. It is to be noted that it is relatively hard to stabilize FeCO_3 in the form of macroscopic crystallites for ruling out size effects. However, we are in the process of exploring systematic size effects in FeCO_3 . We also assert that for systems which are isostructural AFM with $\alpha\text{-Fe}_2\text{O}_3$, such as Cr_2O_3 (which is definitely not a symmetry allowed PzM) and FeCO_3 (for which there are conflicting reports in the literature) the strain in the lattice parameter arising from size effects is likely to stabilize the WFM/PzM phase.^{27,28}

IV. CONCLUSION

In conclusion, we explore two rhombohedral antiferromagnets that are weak ferromagnets and observe an ultra-slow magnetization dynamics and associated with this, a very robust magnetization pinning with unusual magnetic field dependence. These features are intimately related to the weak ferromagnetism arising from spin canting. This spin canting is associated with DMI for the rhombohedral antiferromagnets discussed here. Whether qualitatively similar feature can be observed in other WFM, in which spins are canted but the origin is not DMI driven, is yet to be explored. From present set of data, it is confirmed that the quasi static remanence and its unique magnetic field dependence can be taken as footprints of WFM/PzM systems. This feature is intrinsic in nature and the slow relaxation observed here does not relate with magnetization pinning arising from the glassy phase, magnetocrystalline anisotropy or routine exchange bias. The DMI in WFM phase is clearly connected with the possibility of stress induced moments or piezomagnetism. Finally, piezomagnetism, though not as widely explored or utilized, say as piezoelectricity, can have a variety of applications including those related to FM/AFM interfaces, in which the FM moment can be pinned by a PzM, and the effect should be tunable by stress alone.

V. ACKNOWLEDGMENTS

Authors thank Sunil Nair (IISER Pune) for SQUID magnetization measurements. AB acknowledges Department of Science and Technology (DST), India for funding support through a Ramanujan Grant and the DST Nanomission The-

matic Unit Program. SWC is funded by the Gordon and Betty Moore Foundations EPIQS Initiative through Grant GBMF4413 to the Rutgers Center for Emergent Materials.

Authors thank the DST and Saha Institute of Nuclear Physics, India for facilitating the experiments at the Indian Beamline, Photon Factory, KEK, Japan.

* ashna@iiserpune.ac.in

- ¹ I. E. Dzyaloshinskii, *JETP* **32**, 1259 (1957).
- ² I. E. Dzyaloshinskii, *JETP* **33**, 807 (1957).
- ³ I. Dzyaloshinsky, *Journal of Physics and Chemistry of Solids* **4**, 241 (1958).
- ⁴ T. Moriya, *Phys. Rev.* **120**, 91 (1960).
- ⁵ U. K. Rossler, A. N. Bogdanov, and C. Pfleiderer, *Nature* **442**, 797 (2006).
- ⁶ Y. Onose, T. Ideue, H. Katsura, Y. Shiomi, N. Nagaosa, and Y. Tokura, *Science* **329**, 297 (2010).
- ⁷ M. Z. Hasan and C. L. Kane, *Rev. Mod. Phys.* **82**, 3045 (2010).
- ⁸ Y. Yamasaki, H. Sagayama, T. Goto, M. Matsuura, K. Hirota, T. Arima, and Y. Tokura, *Phys. Rev. Lett.* **98**, 147204 (2007).
- ⁹ B. Binz, A. Vishwanath, and V. Aji, *Phys. Rev. Lett.* **96**, 207202 (2006).
- ¹⁰ C. L. Kane and E. J. Mele, *Phys. Rev. Lett.* **95**, 226801 (2005).
- ¹¹ J. Sinova and I. Zutic, *Nature Materials* **11**, 368 (2012).
- ¹² V. Barthem, C. Colin, H. Mayaffre, M. Julien, and D. Givord, *Nature Communications* **4**, 2892 (2013).
- ¹³ I. Gross, L. J. Martínez, J.-P. Tetienne, T. Hingant, J.-F. Roch, K. Garcia, R. Soucaille, J. P. Adam, J.-V. Kim, S. Rohart, A. Thiaville, J. Torrejon, M. Hayashi, and V. Jacques, *Phys. Rev. B* **94**, 064413 (2016).
- ¹⁴ J. Gayles, F. Freimuth, T. Schena, G. Lani, P. Mavropoulos, R. A. Duine, S. Blügel, J. Sinova, and Y. Mokrousov, *Phys. Rev. Lett.* **115**, 036602 (2015).
- ¹⁵ A. B. Romanov, *Soviet Physics JETP* **11**, 786 (1960).
- ¹⁶ A. S. Borovik-Romanov, *Zh. Eksp. Teor. Fiz.* **38**, 1088 (1960).
- ¹⁷ V. Andratskii and A. S. Borovik-Romanov, *JETP* **687**, 1036 (1966).
- ¹⁸ A. S. Borovik-Romanov, *Ferroelectrics* **162**, 153 (1994).
- ¹⁹ R. R. Birss, *Symmetry and Magnetism* (New York: North-Holland Pub. Co., 1964).
- ²⁰ D. Halley, N. Najjari, H. Majjad, L. Joly, P. Ohresser, F. Scheurer, C. Ulhaq-Bouillet, S. Berciaud, B. Doudin, and Y. Henry, *Nature Communications* **5**, 3167 (2014).
- ²¹ J. Sandonis, J. Baruchel, B. Tanner, G. Fillion, V. Kvardakov, and K. Podurets, *Journal of Magnetism and Magnetic Materials* **104**, 350 (1992).
- ²² S. A. J. Kimber and J. P. Attfield, *J. Mater. Chem.* **17**, 4885 (2007).
- ²³ T. G. Phillips, R. L. Townsend, and R. L. White, *Phys. Rev. Lett.* **18**, 646 (1967).
- ²⁴ T. G. Phillips, R. L. Townsend, and R. L. White, *Phys. Rev.* **162**, 382 (1967).
- ²⁵ J. Kushauer, W. Kleemann, J. Mattsson, and P. Nordblad, *Phys. Rev. B* **49**, 6346 (1994).
- ²⁶ S. Sahoo and C. Binek, *Philosophical Magazine Letters* **87**, 259 (2007).
- ²⁷ A. Bajpai, R. Klingeler, N. Wizen, A. K. Nigam, S.-W. Cheong, and B. Bchner, *Journal of Physics: Condensed Matter* **22**, 096005 (2010).
- ²⁸ A. Bajpai, Z. Aslam, S. Hampel, R. Klingeler, and N. Grobert, *Carbon* **114**, 291 (2017).
- ²⁹ A. Michels, D. Mettus, D. Honecker, and K. L. Metlov, *Phys. Rev. B* **94**, 054424 (2016).
- ³⁰ M. Lisunova, N. Holland, O. Shchepelina, and V. V. Tsukruk, *Langmuir* **28**, 13345 (2012).
- ³¹ X. Liu, J. Zhang, S. Wu, D. Yang, P. Liu, H. Zhang, S. Wang, X. Yao, G. Zhu, and H. Zhao, *RSC Adv.* **2**, 6178 (2012).
- ³² X. Liu, H. Wang, C. Su, P. Zhang, and J. Bai, *Journal of Colloid and Interface Science* **351**, 427 (2010).
- ³³ S. Mørup and C. Frandsen, *Phys. Rev. Lett.* **92**, 217201 (2004).
- ³⁴ M. J. Benitez, O. Petravic, H. Tüysüz, F. Schüth, and H. Zabel, *Phys. Rev. B* **83**, 134424 (2011).
- ³⁵ M. J. Benitez, O. Petravic, E. L. Salabas, F. Radu, H. Tüysüz, F. Schüth, and H. Zabel, *Phys. Rev. Lett.* **101**, 097206 (2008).
- ³⁶ L. Néel, *Rev. Mod. Phys.* **25**, 58 (1953).
- ³⁷ K. Binder and A. P. Young, *Rev. Mod. Phys.* **58**, 801 (1986).
- ³⁸ J. Mattsson, C. Djurberg, and P. Nordblad, *Phys. Rev. B* **61**, 11274 (2000).
- ³⁹ M. Suzuki, I. S. Suzuki, and M. Matsuura, *Phys. Rev. B* **73**, 184414 (2006).
- ⁴⁰ In SQUID magnetometers, even in $H = 0$, there can be some residual magnetic field arising from the superconducting coil. The magnitude of this residual field can be 5 to 10 Oe and its sign can be arbitrary. The vanishingly small value of remanence at $H = 30$ kOe also sets the base line for any artifacts arising from such residual fields.